

Throughput Requirements for RAN Functional Splits in 3D Networks

MohammadAmin Vakilifard, Tim Düe, Mohammad Rihan, Maik Röper,
Dirk Wübben, Carsten Bockelmann, Armin Dekorsy

Department of Communications Engineering, University of Bremen, Bremen, Germany.
{vakilifard, duee, elmeligy, roeper, wuebben, bockelmann, dekorsy}@ant.uni-bremen.de

Abstract—The rapid growth of non-terrestrial communication necessitates its integration with existing terrestrial networks, as highlighted in 3GPP Releases 16 and 17. This paper analyses the concept of functional splits in 3D networks. To manage this complex structure effectively, the adoption of a Radio Access Network (RAN) architecture with Functional Split (FS) offers advantages in flexibility, scalability, and cost-efficiency. RAN achieves this by disaggregating functionalities into three separate units. Analogous to the terrestrial network approach, 3GPP is extending this concept to non-terrestrial platforms as well. This work presents a general analysis of the requested Fronthaul (FH) data rate on the feeder link between a non-terrestrial platform and the ground-station in the Uplink (UL) for two typical Non-Terrestrial Network (NTN) scenarios, Low Earth Orbit (LEO) satellite and High Altitude Platform Station (HAPS). One of the trade-offs for each split option is between the FH data rate and the resulting complexity based on the use case scenario. Since non-terrestrial nodes face more limitations regarding power consumption and complexity onboard in comparison to terrestrial ones, the throughput requirements and suitability of different functional split options must be investigated for this use case as well.

Index Terms—Functional Split (FS), 3D Networks, Non-Terrestrial Communication, 3GPP, Fronthaul Throughput, NTN

I. INTRODUCTION

Current terrestrial networks face limitations in achieving complete coverage due to restricted coverage areas and geographical barriers. Network outages during natural disasters can further disrupt critical operations, jeopardizing lives and property [1], [2]. Three-dimensional (3D) wireless communication networks represent the next frontier in network deployment. These networks leverage a layered approach, integrating space-, air-, and terrestrial-based communication links to achieve seamless and ubiquitous coverage. As we approach the 2030s, the anticipated roll-out of 6G, full integration of non-terrestrial communication links becomes crucial [3]. This includes satellites, mega-constellations in LEO, and airborne

This research was supported in part by the German Federal Ministry of Education and Research (BMBF) within the projects Open6GHub under grant number 16KISK016 and 6G-TakeOff under grant number 16KISK068 as well as the European Space Agency (ESA) under contract number 4000139559/22/UK/AL (AComS).

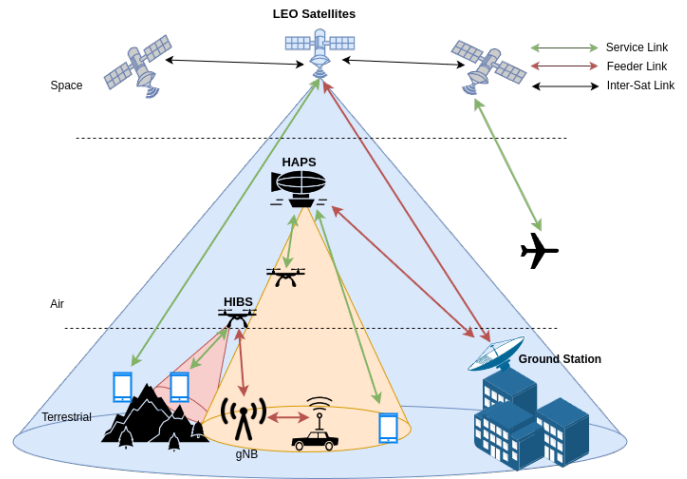


Fig. 1. 3D Network architecture, composed of LEO satellites, HAPS and UAV as two form of HIBS with the different beam size of each Non terrestrial node on the ground.

platforms such as High Altitude Platform Station (HAPS) and Unmanned Aerial Vehicles (UAVs) working in tandem with terrestrial networks. The high number of potential gNodeB (gNB) nodes due to non-terrestrial integration necessitates flexibility, robustness, cost-effectiveness, and energy efficiency in these new platforms. Consequently, integrating the concept of Functional Split (FS) with non-terrestrial platforms becomes a critical step towards achieving these goals.

The 3GPP Release 15 introduced the adaptable design for the 5G Radio Access Network (RAN) [4]. This design disaggregates the traditional gNB into three logical nodes: the Radio Unit (RU), Distributed Unit (DU), and Center Unit (CU). So far, 3GPP has introduced in principle eight FS options for RAN in terrestrial networks. In the recent years, the O-RAN alliance, another major player, has focused on physical layer splits and presented its own split based architecture of RAN [5].

Different FS options necessitate varying data rates to transmit the same information between nodes as calculated in [6]. These requirements depend on the deployment scenario

and the characteristics of the interface between the split components. 3GPP has addressed the calculation of FH data rate for LTE and New Radio (NR) in [7]–[9] in their respective specifications. So far, most investigations on FS are performed for terrestrial networks [10], [11], while some papers such as [28] and [29] has analyzed the feasibility of RAN functional split in NTN but by considering FH data rate based on the terrestrial network. Therefore specific constraints in NTN scenario are not completely investigated.

This paper proposes a general formulation to determine the FH data rate needed for implementing FS in the Uplink (UL) with non-terrestrial platforms. The FH data rate describes the amount of data needed to be transmitted between a terrestrial and non-terrestrial node during on the feeder link. Additionally, we suggest which of the investigated physical layer split options is most suitable for non-terrestrial nodes.

II. FUNCTIONAL SPLIT FOR 3D NETWORKS

A. 3D Networks

3D Networks extend conventional terrestrial networks with air- and space-borne network nodes, as depicted in Fig. 1. The NTN nodes, i.e., the air- and spaceborne network nodes such as LEO satellites and HIBS, provide connectivity between a terrestrial User Equipment (UE) and a ground station, which is connected to the Core Network.

Accordingly, we distinguish between two communication links:

- 1) Service Link: The communication link connecting UE and the non-terrestrial platform, which hosts some part of RAN functionalities.
- 2) Feeder Link: The communication link between the non-terrestrial platform and the ground which host the rest of RAN functionalities and is connected to the Core Network.

B. Functional Split in Terrestrial Network

3GPP introduced in principle eight FS options for a gNB, as depicted in Fig. 2, whereas options 4 and 5 are deemed impractical for implementation [5]. O-RAN also has introduced architectures, which decompose network functions into distinct components that can be implemented on various hardware, which have garnered increased attention [14]. O-RAN primarily concentrates on option 7 of the FS proposed by 3GPP, with a focus on separating the RU and DU functions [15]. Depending on specific FSs, there is a trade-off between computational complexity onboard of the platform and data rate demand on interface link. Other trade-offs, such as timing requirements, latency restrictions, and link performance, also are of high importance but not in the context of this paper.

C. Functional Split for Non-Terrestrial Network

3GPP has introduced three non-terrestrial access architectures for satellites, including the transparent payload-based, where the satellite acts as a relay between the user and the Core [16]; a regenerative payload-based, where the gNB is fully implemented on the satellite board [5]; and a regenerative

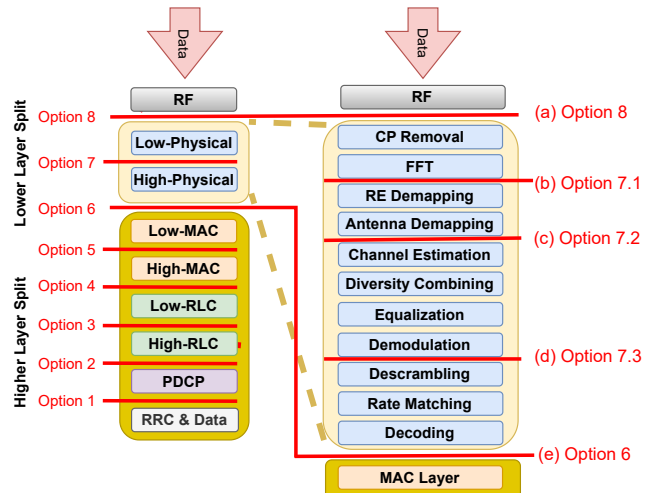


Fig. 2. 3GPP FS in UL. On the left there are eight FS options introduced by 3GPP, and on the right there are lower layer split options in baseband processing unit.

satellite-based gNB-DU, which considers split option 2 with the complete RU and DU implemented onboard the satellite [17]. O-RAN has not yet officially considered its architecture for NTN, while in [18] O-RAN based NTN has been investigated.

While the 3GPP has currently designated option 2 for NTNs, the push towards a unified 3D network with diverse communication elements necessitates exploring lower layer split options [19], [20] to reduce complexity by not realizing full gNB on the non-terrestrial nodes. For NTN, such lower layer splits lead to a reduced complexity of the NTN nodes.

The reasons why 3GPP has so far not favored lower layer splits for NTN are timing issues and latency. In terrestrial networks, the necessity to quickly adjust to changes in Channel State Information (CSI) drives the demand for reduced latency in lower layer splits, as e.g. beamforming requires precise CSI.

However, if the position of the ground station node and user nodes are known sufficiently well to the non-terrestrial node, the requirements for precise CSI reduce significantly. As the beamforming on space-borne platforms mainly sets the beam on specific positions on the Earth's surface and does not adjust to fast changing channel conditions, the positional information can be used to infer the CSI information as shown in [21], relaxing the latency requirements on the feeder link, which results in making the FS possible.

The main challenges regarding FS for non-terrestrial platforms can be listed as:

- 1) Timing requirements fulfilling 3GPP constraints.
- 2) Level of computational complexity needed onboard, which correlates with energy consumption and cost;
- 3) High FH data rate over the feeder-link;
- 4) Constrained memory capacity requirements onboard.

As seen in Fig. 2, split options are classified into high layer and low layer splits. High layer splits enable effective data storage on non-terrestrial systems by reducing memory

requirements as a result of more processing operations. High layer FS reduce the needed FH data rate and need higher timing requirements. However, they also raise the complexity and power consumption of the baseband processing. Lower FS, on the other hand, may be advantageous for non-terrestrial nodes since they reduce hardware complexity, as this study explores with options 8, 7, and 6. The necessity for a balanced approach in the design and implementation of access architectures for non-terrestrial platforms is highlighted by this trade-off.

III. SYSTEM MODEL

By considering the regenerative access architecture as baseline and prior works of [22], [23] and [24], we focus on the Uplink (UL) case from a UE to the Core Network through a non-terrestrial node. Fig. 2 shows the block diagram of the baseband processing chain for each FS option from 8 to 6 and their involving functionalities. By moving from FS option 8 towards 6, the FH data rate and memory requirements are reduced, but the computational complexity and power consumption will increase.

We consider a non-terrestrial communication node operational at the height of h_C , so that the number of cells on the ground it can cover is N_C . Each cell is covered by N_B beams. Each beam is created by L number of antenna elements. Therefore, the total number of active antennas is $N_{\text{ant}} = N_C \cdot N_B \cdot L$. We perform our analysis for two scenarios:

- Scenario 1 (SC1): A LEO satellite at the height $h_C = 600$ km covers $N_C = 19$ cells based on [16]
- Scenario 2 (SC2): A HIBS at the height $h_C = 10$ km covering $N_C = 8$ cells based on [22].

Without loss of generality and for the sake of comparison, we consider based on [4], [16] and [25] that both LEO satellite and the HIBS use the same array of antennas and one beam per cell is considered ($N_B = 1$). Each beam can support a bandwidth of B_{BW} . The total number of covered UEs in each beam is:

$$N_{\text{UE}} = A_{\text{Beam}} \cdot \rho_{\text{UE}} \quad (1)$$

where:

- A_{Beam} is the beam foot print size on ground equal to $\pi \cdot r_{\text{Beam}}^2$ which r_{Beam} is the beam radius as function of platform height, its equivalent antenna aperture and carrier frequency band. Therefore we have r_{BeamSC1} equal to 25 km for S band and 10 km for Ka band.
- ρ_{UE} is UEs density per square kilometer $\frac{\text{UEs}}{\text{km}^2}$, which varies depending on the type of communication such as Enhanced Mobile Broadband (eMBB) or massive machine-type communications (mMTC).

Since different altitudes h_C and corresponding values of N_{UE} result in different Signal to Interference and Noise ratio (SINR) and consecutively different Modulation and Coding Scheme, but here in the rest of the paper without loss of generality and sake of simplicity, it is assumed that all covered UEs use the same modulation order M and code rate R_c for both scenarios.

TABLE I
PARAMETERS FOR FH CALCULATIONS

Variable Name	Meaning	Value	
N_C	No. of covered cells	SC1: 19	SC2: 8
B_{BW}	Bandwidth (BW) per beam	S band: 30 MHz	Ka band: 400 MHz
r_{Beam}	Beam radius on the ground	SC1	
		S: 25 km	Ka: 10 km
ρ_{UE}	UEs density	SC2	
		S: 6 km	Ka: 6 km
PR	Reference Peak Rate	eMTC: 500 $\frac{\text{UEs}}{\text{km}^2}$	
		mMTC: 500 $\frac{\text{UEs}}{\text{km}^2}$	
BW_{ref}	Reference bandwidth	eMBB: 0.1 $\frac{\text{UEs}}{\text{km}^2}$	
		S: 2 Mbit/s	Ka: 100 Mbit/s
N_B	No. of beams per cell	S: 0.256 Mbit/s	Ka: 7 Mbit/s
L	No. antenna elements create a beam	S: 5 MHz	Ka: 100 MHz
S	Over sampling rate	1	
Q_T	Quantization in time	2	
Q_F	Quantization in frequency	1 S/s	
τ_{CP}	CP duration	16 bits	
τ_{subframe}	OFDM subframe duration	10 bits	
μ	OFDM numerology	4.688 μs	
η	Utilization factor	1 ms	
N_S	No. symbols	0	
N_{SC}	No. of subcarriers	0.6	
N_{data}	No. of data REs	14	
M	No. of symbols per beam	12	
Q_{LLR}	Quantization per LLR	110	
R_c	Code rate	2 : 256 QAM	
N_L	No. Layer	3 bits	
M_{ref}	Reference modulation order	0.64 for $M = 16$	
ρ_{UL}	Fraction of UEs requesting UL	8	
S_{UL}	Average content size in UL by UEs	2 for $M = 2$ and 4, 4 for $M = 16$, 16 for $M = 64$, 64 for $M = 256$	
		1 for a fully loaded scenario; 0 for an unloaded system	
		30 B based on [8]	

Based on [7] upon reception, each sample after Analog-to-Digital converter is represented by Q_T bits. The service link data rate is calculated by using

$$R_{\text{Service Link}} = N_C \cdot N_B \cdot N_{\text{UE}} \cdot B_{\text{BW}} \cdot L \cdot S, \quad (2)$$

in which S is the over sampling rate. All the example parameters are reported with details in Table I. The values are chosen based on different scenarios in the standard 3GPP TR38.821 [16], [22] and [25].

IV. FRONTHAUL RATE CALCULATION FOR THE FUNCTIONAL SPLIT OPTIONS

In this section, we utilize the general formulation and variable definitions provided in Section III to derive the calculation of the FH data rates of the considered FS options by 3GPP as shown in Fig. 2. Additionally, we discuss their respective advantages and disadvantages.

A. Option 8: Time Domain

In this FS option, only RF-related processes are performed on the non-terrestrial node. These include analog-to-digital conversion and quantization at each antenna element's output. Assuming perfect sampling, no oversampling occurs, so data volume doesn't increase. The received signal is quantized in the time domain using Q_T bits per sample per axis (In-Phase and Quadrature), resulting in each sample being represented by $2 \cdot Q_T$ bit. Considering the maximum transmission bandwidth in $R_{\text{Service Link}}$ from cells to the non-terrestrial platform we can write:

$$R_{\text{Opt8}} = R_{\text{Service Link}} \cdot 2 \cdot Q_T. \quad (3)$$

The data to be transmitted over the FH are I/Q samples, which in case of even no user data (no load) still exists. The primary advantage of option 8 lies in its low onboard complexity leading to reduced power consumption attributed to minimal signal processing. However, a notable drawback is the very high FH data rate on the feeder link, as Q_T (16 bits is a typical value) is relatively high for time-domain signal to a high represent the signals adequately.

B. Option 7.1: Frequency Domain w/o CP

This option involves the removal of symbols designated for OFDM Cyclic Prefix (CP). The CP length is a process dependent variable, represented by the OFDM numerology μ for each subframe. The duration of a single subframe τ_{subframe} for NR is standardized to 1 ms [5]. The total duration of the CPs per frame is $N_S \cdot (\mu + 1) \cdot \tau_{\text{CP}}$. After the CP removal, the signal is transformed to the frequency domain using a Fast Fourier Transform (FFT). We can quantize level of the symbols in the frequency domain as Q_F . Q_T and Q_F denote the number Q-levels if messages are transmitted over the FH. In frequency domain less bits are sufficient therefore $Q_F < Q_T$ and typically is $Q_F = 10$ bits. The rate for this option can be expressed as

$$R_{\text{Opt7.1}} = R_{\text{Opt8}} \cdot \frac{\tau_{\text{subframe}}}{\tau_{\text{subframe}} + N_S \cdot (\mu + 1) \cdot \tau_{\text{CP}}} \cdot \frac{Q_F}{Q_T}. \quad (4)$$

This FS results in the reduction of data rate, as both terms are less than 1. Option 7.1 does add complexity onboard, however, it is still relatively low, as the required operations are basic and efficient hardware solutions exist.

C. Option 7.2: Resource-Element Demapping

This option follows a procedure outlined in [26], where the maximum number of layers is $N_L = 8$ which is the same for NTN as well. Resource Element (RE) demapping eliminates unused resource elements in the received signals from users which is determined by the system's actual load, referred to as utilization factor η , which includes antenna logical ports demapping according to [27]. The data rate of option 7.2 can be written:

$$R_{\text{Opt7.2}} = R_{\text{Opt7.1}} \cdot \eta. \quad (5)$$

The inclusion of η leads to a reduction in the FH rate, as we now forward only the used REs, therefore this option depends on the actual load of the system. This FS option is very significant in scenarios with very low utilization, expressed by $\eta \ll 1$. The value of η highly depends on the scenario. This FS is currently favored by 3GPP for terrestrial networks and could be an effective option for non-terrestrial platforms as well.

D. Option 7.3: Equalization and Demodulation

This option introduces a split in UL motivated by FS option 7.3 for terrestrial networks of the 3GPP. This FS option includes all the functionalities requiring CSI, which are channel estimation, diversity combining, equalization, and demodulation. Therefore, option 7.3 omits the necessity to forward CSI to the ground station.

Here, the pilots and other reference symbols like Sounding Reference Signals (SRS) and Phase-tracking Reference Signals (PTRS), employed to gain CSI, can be removed, decreasing the FH data rate. Equalization is performed for each beam, which reduces the throughput by a factor of $\frac{1}{L}$ after combining multiple antenna streams into a single beam.

After demodulation, there are $\log_2 M$ code bits per symbol, each bit is expressed by Log-Likelihood Ratio (LLR) with Q_{LLR} bit. The resulting FH data rate is given by

$$R_{\text{Opt7.3}} = R_{\text{Opt7.2}} \cdot \frac{N_{\text{Data}}}{N_S \cdot N_{\text{SC}}} \cdot \frac{1}{L} \cdot \frac{\log_2 M}{Q_F} \cdot Q_{\text{LLR}}. \quad (6)$$

Here, N_{Data} represents all REs dedicated solely for data transmission, whereas $N_S \cdot N_{\text{SC}}$ represents the total number of REs after the CP removal.

By increasing modulation order M , the FH data rate increases as well, as Q_{LLR} bits are forwarded for each code bit. However, novel compression approaches based on the Information Bottleneck Method (IBM) have been designed successfully to limit the information loss by quantization while keeping the relevant information [28]. It is expected, that this technique can significantly reduce the resulting FH rate, while meeting the End-to-End performance constraints [29]. However, the application of IBM-based quantization is beyond the scope of this paper.

The downsides are the considerably increased computation resources and power consumption's. Nonetheless, with the emergence of high-performance Artificial Intelligence-based solutions for channel estimation and equalization, this split shows promising potential, especially for non-terrestrial nodes.

E. Option 6: Decoding

This option involves several key steps: descrambling, rate dematching, and decoding, which prepare the data for transmission via the feeder link to the ground. Descrambling reorders the data to its original form, and rate dematching adjusts the data sequence to match the original transmission rate without altering the total number of bits. The decoding process, which is particularly crucial, takes LLR bits, Q_{LLR} , and reconstructs the original information bits. This process is performed using a specific decoding method (like Low density parity check (LDPC) decoding), which operates at a code rate R_c . The decoding step reduces the number of remaining bits in the data stream, as it compresses the data by a factor related to the code rate. This is expressed as:

$$R_{\text{Opt6}} = R_{\text{Opt7.3}} \cdot \frac{1}{Q_{\text{LLR}}} \cdot R_c. \quad (7)$$

Option 6 offers the advantage of markedly reducing the FH data rate. However, the functionalities involved, particularly the decoding process, entail a considerable degree of computational complexity and energy consumption onboard.

F. Option 2: High-Layer DU/CU split

FS Option 2, proposed by 3GPP as a higher layer split between the CU and DU at the output of Radio Link Control (RLC), is recommended for regenerative scenarios, including NTN, and can be considered a baseline because it is currently the only functional split specifically suggested by 3GPP for such applications. In this option, nearly all signal processing is performed on the platform, leading to significantly lower FH requirements and more relaxed latency constraints, but at

the cost of increased onboard complexity. The FH data rate on the feeder link can be calculated similar to [8] as:

$$R_{\text{Opt2}} = PR \cdot \frac{B_{\text{BW}}}{BW_{\text{ref}}} \cdot \frac{N_{\text{L}}}{N_{\text{Lref}}} \cdot \frac{M}{M_{\text{ref}}} + \text{signaling} \quad (8)$$

in which $N_{\text{Lref}} = 1$ as reference number of layer based on [10]. $\text{signaling} = N_{\text{UE}} \cdot p_{\text{UL}} \cdot S_{\text{UL}} \cdot N_{\text{L}}$, is the amount of data as function of load on the system (as p_{UL} shows the percentage of users requesting UL) and the average size of content in UL by users.

V. RESULTS

In this section we present the results of the analysis for the FH data rate of each FS option formulated in Section IV for two described scenarios in Section III.

Fig. 3, shows the needed FH data rates for each functional split (FS) option for the two scenarios of LEO satellite at $h_{\text{C}} = 600$ km and HIBS at $h_{\text{C}} = 10$ km for the eMBB service type in case of S and Ka bands, while Fig. 4 shows the same for mMTC service type. The platform altitude, service type, and B_{BW} directly influence the number of users that can be covered, which in turn affects the required FH data rate on the feeder link.

The needed FH data rate for a higher altitude node like LEO satellite in SC1 is much higher than HIBS in SC2, due to covering more cells and therefore users. For mMTC results in Fig. 4. for both scenarios and B_{BW} the FS options 8 to 6 all show much higher data rate in comparison to eMBB in Fig. 3 due to denser presence of users.

As anticipated, option 8 demands the highest data rate for all cases as time-domain IQ samples for all received signals, independent from the load on the system, are forwarded to ground-station on the feeder link. FS options 7.1, 7.2 and 7.3 reduce the data rate in Fig. 3 in average by 41.3%, 64.8% and 89.7%, respectively, w.r.t option 8 by not adding much more extra complexity on the board. Option 6 hosts the decoder can reduce the rate for both frequency bands by 97.9% and 83.34% w.r.t option 8 and 7.3 respectively. The values are closely the same for mMTC service type in Fig. 4. For option 2 as baseline we can see reduction of 99.46% and 97.45% w.r.t option 8 and 7.3 respectively, in cost of adding more functionalities on board. We can conclude that FS option 6 can be a potential candidate for non-terrestrial nodes, in comparison to option 2 with lower complexity and cost. Depends on the type of service FS option 7.3 can come in the second place, mainly for eMBB.

We can say that for mMTC service option 2 shows the most applicable FH data rate, while option 6 in S band also is feasible, especially since the beam diameter is wider than Ka band means more users can be covered.

In Fig. 5, the required FH data rates for FS Options 7.3, 6, and 2 are shown as a function of different modulation orders (M) and corresponding coding rates (R_{c}) for eMBB services in scenario 2, where the HIBS is positioned at $h_{\text{C}} = 10$ km. The R_{c} for each M is selected to maximize spectral efficiency, according to [30]. In case of air-born nodes such as HAPS

or drones, due to their lower altitude and longer visibility in comparison to LEO satellites, the non-terrestrial node based on the request of ground station can ask users to change their modulation and coding scheme (MCS) based on the received signal SINR to perform link adaptation on the service link. This leads to change in the FH data rate on the feeder link. Option 7.3 increases more by higher modulation order due to the need of sending demodulated bits multiply by the Q_{LLR} factor. option 6 and 2 show close FH data rate in lower (M, R_{c}), while after 64 QAM the gap increases, due to the higher code rate. Option 7.3 with lower complexity in comparison to option 6 and 2, in both S band and Ka band, can be a suitable option even for higher modulation order especially in case of eMBB service type for air-born nodes. This can be extended as a future work for case of other non-terrestrial nodes such as LEO satellites by performing a link-level simulation.

VI. CONCLUSION

This paper investigates the concept of FS in the physical layer for components of 3D Networks. We have derived the required FH data rate in UL for non-terrestrial objects. Based on our results, we have shown that the data rates depend on key parameters, which we can optimized based on the specific requirements of a scenario, such as minimizing the FH data rate versus increasing the computational complexity w.r.t the option 2 CU-DU split as baseline. Our formulation gives the flexibility to extend the analysis for different types of use cases as we analyzed the for different heights, two different type of service and frequency bands of S and Ka band. The selection of FS option mainly depends on the use case specifically type of service and frequency band. As shown in case of eMBB service type option 7.3 can be promising option, while for more users to be covered (higher h_{C} or service type of mMTC) option 6 and option 2 are more feasible.

REFERENCES

- [1] S. Mahboob, L. Liu. "A Tutorial on AI-Enabled Non-Terrestrial Networks in 6G.", arXiv preprint arXiv:2303.01633, 2023.
- [2] Y. Wu, S. Singh, T. Taleb, A. Roy, H. S. Dhillon, M. R. Kanagarathinam, A. De, "6G mobile wireless networks", Berlin, Germany, Springer, 2021.
- [3] G. Geraci, D. López-Pérez, M. Benzaghta, S. Chatzinotas, "Integrating Terrestrial and Non-Terrestrial Networks: 3D Opportunities and Challenges", IEEE Communications Magazine, vol. 61, no. 4, April 2023.
- [4] 3GPP TR 38.811 v15.2.0: "Study on New Radio (NR) to support non-terrestrial networks (Release 15)".
- [5] S. Sirotkin, "5G Radio Access Network Architecture: The Dark Side of 5G.", John Wiley & Sons, 2020.
- [6] D. Wübben, P. Rost, J. S. Bartelt, M. Lalam, V. Savin, M. Gorgoglione, A. Dekorsy, G. Fettweis, "Benefits and impact of cloud computing on 5G signal processing: Flexible centralization through cloud-RAN", IEEE signal processing magazine, 2014.
- [7] 3GPP R3-162102: "CU-DU split: Refinement for Annex A (Transport network and RAN internal functional split)" Sophia Antipolis, France, 10th to 14th, October 2016.
- [8] 3GPP TR 38.801 v14.0.0: "Study on new radio access technology: Radio access architecture and interfaces (Release 14)".
- [9] 3GPP TR 38.816 v15.0.0: "Study on Central Unit (CU) - Distributed Unit (DU) lower layer split for NR (Release 15)".
- [10] S. Lagén, L. Giupponi, A. Hansson, X. Gelabert, "Modulation Compression in Next Generation RAN: Air Interface and Fronthaul Trade-offs", IEEE Communications Magazine, vol. 59, no. 1, January 2021.

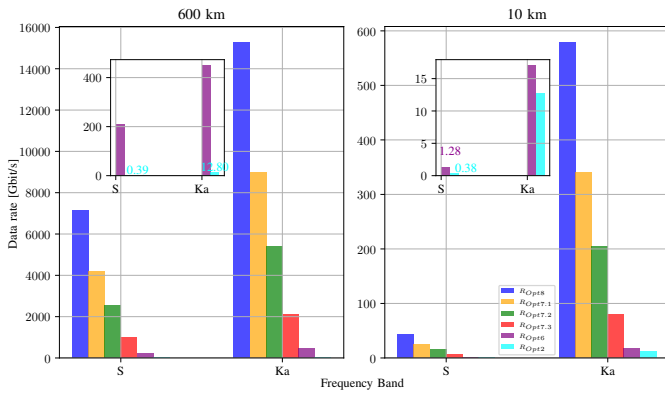


Fig. 3. eMBB service type with $M = 16$ QAM and $R_c = 0.64$.

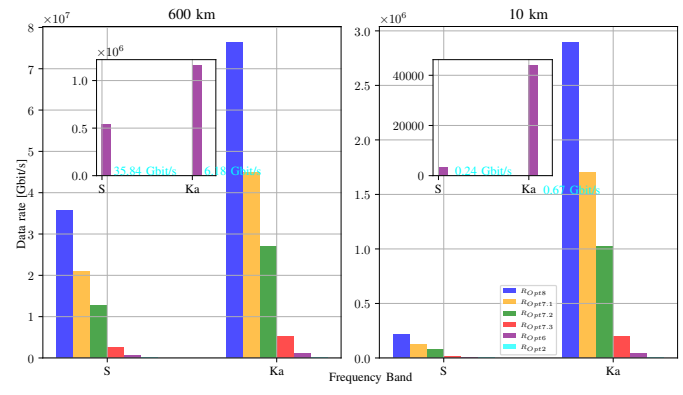


Fig. 4. mMTC service type with $M = 4$ QAM and $R_c = 0.66$.

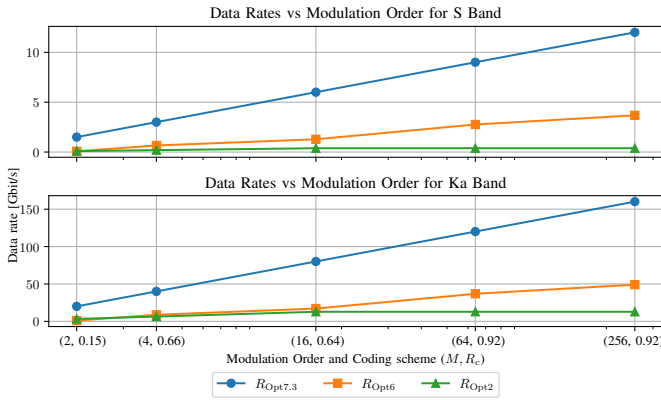


Fig. 5. Scenario 2 needed FH data rate of split options 7.3, 6 and 2 vs modulation order and Coding scheme pair for eMBB service type. The X-Axis is in log-scale

[11] L. M. P. Larsen, A. Checko, H. L. Christiansen, "A Survey of the Functional Splits Proposed for 5G Mobile Crosshaul Networks", IEEE Communications Surveys & Tutorials, vol. 21, no. 1, Firstquarter 2019.

[12] Seeram, S.S.S.G., Feltrin, L., Ozger, M., Zhang, S. and Cavdar, C., 2024. Feasibility Study of Function Splits in RAN Architectures with LEO Satellites. arXiv preprint arXiv:2404.09186.

[13] Campana, R., Amatetti, C. and Vanelli-Coralli, A., 2023. RAN Functional Splits in NTN: Architectures and Challenges. arXiv preprint arXiv:2309.14810.

[14] E. Municio, G. Garcia-Aviles, A. Garcia-Saavedra and X. Costa-Pérez, "O-RAN: Analysis of Latency-Critical Interfaces and Overview of Time Sensitive Networking Solutions", IEEE Communications Standards Magazine, vol. 7, no. 3, September 2023.

[15] E. Sarikaya, E. Onur, "Placement of 5G RAN Slices in Multi-tier O-RAN 5G Networks with Flexible Functional Splits", 17th Int. Conf. on Net. and Service Manag. (CNSM), Izmir, Turkey, 2021.

[16] 3GPP TR 38.821 v16.1.0: "Solutions for NR to support non-terrestrial networks (NTN) (Release 16)".

[17] M. R. Elmeligy, T. Düe, M. Vaklifard, D. Wübben, A. Dekorsy, "RAN Functional Split Options for Integrated Terrestrial and Non-Terrestrial 6G Networks", 11th International Japan-Africa Conference on Electronics, Communications, and Computations (JAC-ECC), Alexandria, Egypt, 2023.

[18] R. Campana, C. Amatetti, A. Vanelli-Coralli, "O-RAN based Non-Terrestrial Networks: Trends and Challenges", Joint European Conference on Networks and Communications & 6G Summit (EuCNC/6G Summit), Gothenburg, Sweden, 2023.

[19] S. Bonafini, C. Sacchi, F. Granelli, S. T. Arzo, M. Devetsikiotis, K. Kondepu, "HW/SW Development of Cloud-RAN in 3D Networks:

Computational and Energy Resources for Splitting Options", IEEE Aerospace Conference, Big Sky, MT, USA, 2023.

[20] R. Bassoli, F. Granelli, "Pico Satellites for Cloud Radio Access Network", IEEE 2nd 5G World Forum (5GWF), Dresden, Germany, 2019.

[21] M. Röper, B. Matthiesen, D. Wübben, P. Popovski and A. Dekorsy, "Beamspace MIMO for Satellite Swarms," IEEE Wireless Communications and Networking Conference (WCNC), Austin, TX, USA, 2022.

[22] Y. Xing, F. Hsieh, A. Ghosh, T. S. Rappaport, "High altitude platform stations (HAPS): Architecture and system performance", IEEE 93rd Vehicular Technology Conference (VTC2021-Spring), 04.2021.

[23] J. C. Borromeo, K. Kondepu, N. Andriolli, L. Valcarengi, R. Bassoli, F. H. P. Fitzek, "5G NR Support for UAV-Assisted Cellular Communication on Non-Terrestrial Network", 27th European Wireless Conference, Dresden, Germany, 2022.

[24] S. Bonafini, C. Sacchi, R. Bassoli, F. Granelli, K. Kondepu, F. H. P. Fitzek, "An Analytical Study on Functional Split in Martian 3-D Networks", IEEE Transactions on Aerospace and Electronic Systems, 2022.

[25] Euler, S., Lin, X., Tejedor, E. and Obregon, E., 2022. High-altitude platform stations as international mobile telecommunications base stations: A primer on HIBS. IEEE Vehicular Technology Magazine, 17(4), pp.92-100.

[26] 3GPP TR 38.211 v16.2.0: "5G NR Physical channels and modulation (Release 16)".

[27] 3GPP TS 138 212 V16.2.0: "5G; NR; Multiplexing and channel coding" (Release 16).

[28] S. Hassanpour, T. Monsees, D. Wübben and A. Dekorsy, "Forward-Aware Information Bottleneck-Based Vector Quantization for Noisy Channels," in IEEE Transactions on Communications, vol. 68, no. 12, pp. 7911-7926, 2020.

[29] M. Hummert, S. Hassanpour, D. Wübben and A. Dekorsy, "Deep Learning-Based Forward-Aware Quantization for Satellite-Aided Communications via Information Bottleneck Method", 2024 EuCNC & 6G Summit, Antwerp, Belgium, 2024.

[30] 3GPP TS 38 214 V18.3.0: "5G; NR; Physical layer procedures for data" (Release 15).